# Morban's thesis

Marco Orban

# Chapter 1

# Introduction

## 1.1 Background

Ostheoarthritis is a very common type of arthritis that causes pain, swelling and stiffness in various body parts such as the hands, hips, back and knees. Over time, it affects bones, cartilage and other tissues, and is common in adults over the age of 45. Knee ostheoarthritis, also known as degenerate joint disease of the knee, is a type of ostheoarthritis that is predominantly seen in the elderly, and is a progressive disease that results in knee stiffness and swelling and pain after sitting or staying still for a long time. Although this disease can be treated, but not cured, with physical therapy and medications that slow down its progression, severe knee ostheoarthritis can only be resolved by means of surgery, in which the whole knee is replaced by a prothesis. Total knee arthoplasty (TKA), also called total knee replacement (TKR) is a very effective and consistently successful surgery that provides good outcomes for patients suffering from end-stage knee ostheoarthritis. TKR results in greatly improved pain relief and better quality of life for patients [1].

Since ostheoarthritis is a disease that is most commonly seen in the elderly, as the percentage of elderly people in developed countries around the world increases, the prevention and treatment of diseases like ostheoarthritis become more important

from a public health persepective. In particular, Taiwan has already exceeded the threshold (14%) of the definition of aged society established by the United Nations, with 3.983 million citizens over the age of 65, acounting for 17.18% of the population [2]. Additionally, it has been estimated that Taiwan's National Health Insurance already spens 5% of its total expenditure on TKR every year, and the incidence of TKR has already tripled in the period between 1996 and 2010 [3].

There has been a growing interest of using additivie manufacturing (AM) for the manufacture of the prosthetics used in TKA, since additive manufacturing is a technology well suited for the creation of custom, lightweight components with complex geometries, while also producing less material compared with other methods of manufacture [4]. Even though additive manufacturing offers many advantages for the production of structures tailored to each individual patient, one of the major obstacles that stands in the way of a more widespread adoption are the high costs of AM. One way to reduce the cost of the total procedure is by reducing the amount of material used, which can also be accomplished by reducing the amount of scrap from the fabricated parts. In additive manufacturing, much of the scrap comes from discarding the support structures that the components require for manufacturing, and thus making smaller support components or using smaller volumes for them would be a valid strategy to further reduce the cost of additive manufacturing components. The total deformation of the part after manufacture is also an important factor to consider, since additional costs can be incured from the addition or removal of material from the manufactured component by means of machining, in order to meet tolareances [4].

# Chapter 2

# Literature Review

What I need to do in the literature review is an introduction, body and conclusion. The introduction should be an overview of the topics that I am going to talk about, and probably introduce the research motivation.

## 2.1 Introduction

Additive manufacturing, also known as 3D printing, is a manufacturing process in which parts are built by stacking layers of material on top of each other until the desired geometry is created. In particular, powdered-bed fusion is a type of additive manufacturing in which the base material is composed of a metallic powdered. A bed is then filled with this powder, and a high-powered laser or electron beam is utilized to selectively add heat to locations of this powdered metal, thus melting it. As the melted portions cool, it leaves a layer of solid material, and the whole component is then built layer by layer in this manner. If a laser is used for manufacturing, the process is then known as laser powder bed fusion (LPBF).

PBF involves the layer-by-layer addition of material in which a heat source selectively melts and fuses regions of a powder bed to form a solid structure. When the material is melted and fused by using a laser, the process is called selective laser melting (SLM). The starting point of selective laser melting is a 2D computer-assisted design

(CAD) model, which is sliced into 2-dimensional pieces, and later uploaded to an SLM machine. The machine then uses the laser to melt layers of powder following the information of the sliced model. At the end of each slice, the layer is left to cool down and solidify, and a new layer of powder is evenly distributed using a coater, and the melting process begins anew, until the final geometry has been reached [5]. The part is then removed from the powder bed where it might then undergo different post-processes, such as removal of supporting structures, heat treatment, or any other additional or removal of material to achieve the required dimensions and tolerances.

Additive manufacturing in general allows for the creation of parts with complex geometries that would otherwise be difficult, time-consuming or too costly to manufacture with other more traditional means of manufacturing such as machining or casting. This can be compared with the manufacture of prosthesis using traditional manufacturing, which relies on the high-volume production of standardized parts and shapes. Due to the ease of creating parts with complex geometries and with shorter lead times, additive manufacturing has had a growing interest from the medical industry for the creation of custom-made implants tailored to an individual patient's anatomy [6] [4]. Additionally, this benefit of creating customized parts also leads to an improvement of patient comfort and better outcomes in orthopedic and surgical applications, as well as enhancing surgical precision and reducing complications of post-operative care [7] [8].

Despite its advantages in creating components with complex free-form 3D geometry, SLM still faces many challenges that limit its application and development. Some of these challenges are related to the development of excessive deformation, thermal stresses, and other mechanical defects such as delamination, distortion and microcracks that result from the great thermal gradients that occur within the component as it is being built, caused by the high heating and cooling rates inherent in the process [9].

Additionally, even though additive manufacturing is a viable alternative for the production of complex-shaped components, its cost can still remain high due to machine, material and process-level expenses. In particular, as a means of creating medical implants for knee-replacement therapy, the high cost of AM limits its usage for revision

procedures, i.e. second or third procedures in which the objective is to replace a failed or uncomfortable component [4]. To solve the problem of high material costs, Laureijs et al. [10] have identified that one of the main driving costs is the price of the powder price. One of the viable options to drive down the price of prosthesis created using additive manufacturing would be to reduce the amount of scrap material involved in the process. Scrap material in additive manufacturing results from discarding the support structures that the part requires as well as any addition or removal of material to the part in post-processing steps to ensure that the part is maintained within tolerances [10].

The support structures alluded to in the previous paragraph refer to the structures that are built alongside the manufactured component that serve to stabilize it during the printing process. These structures are used to aid with supporting overhang areas, which are defined as areas in the structure that are almost horizontal. Support structures can also facilitate the remove of the part from the base plate and other workpieces, and can also aid with thermal diffusion or prevent residual stresses caused by thermal gradients [11].

The design of support structures in additive manufacturing is thus an important consideration, with many factors affecting how the support structure will be built. A well optimized and design support structure will enable the part to be realized, while at the same time using the least amount of material possible to obtain a specified objective. Thermal and mechanical requirements are usually at the forefront of support structure design as they have a direct effect on the quality of the component, although there might be other considerations for the design, such as ease of removability, build time, and material efficiency. Additionally, large portions of surfaces that are almost horizontal and that are unsupported during manufacturing tend to be heavily distorted after manufacturing [12]. At overhang regions, support structures are also required to be as stiff as possible to withstand the weight of the part itself and prevent it from distorting during the building process [13] [14].Another important factor that impacts the design of support structure is the structure's performance to transfer heat away from

the build component, since high thermal conduction can improve the cooling process during fabrication, which helps prevent issues caused by excessive thermal deformation such as thermal residual stresses, thermal dilation, cracks or warping [12] [15].

Topology optimization is a method that is well-suited for the creation and optimization of shapes that satisfy specific constraints while realizing certain objectives [16], and is a well-known technique that has been obtaining more interest from the additive manufacturing community for both the design of the components themselves and for their support structures in additive manufacturing. Topology optimization has been studied for designing parts that either have as little overhang surfaces as possible, thus requiring less supporting structures, or for designing parts that are self-supporting, thus requiring no supporting structures at all. Although this aid considerably in reducing the amount of material used, these approaches do not take into consideration other effects such as the thermal dissipation of the component, or require changing the geometry of the component, thus impacting its functionality [17]. Changes in the geometry of the component might also impose geometrical constraints that can restrict the part's performance [18]. Therefore, instead of using topology optimization to change the shape of the part, much research has been made to apply topology optimization to the design of the support structure itself.

Since topology optimization is one of most popular methods for the design of support structures and the central idea used for this thesis, the following section will consist of an overview of the main ideas and implementation of topology optimization.

## 2.2 Topology optimization

### 2.2.1 Formulation

Topology optimization is an optimization technique that seeks to find the optimal shape within a volume that satisfies certain governing equations while at the same time satisfying specific constraints. This technique is usually utilized for the design of structures

with no preconceived shape. Mathematically speaking, topology optimization seeks to find the optimal distribution of a design variable $\rho$ within a design domain $\Omega$. The placement of $\rho$ will also obey certain governing equations that are valid within the domain, and the existence of this distribution of $\rho$ will also depend on a certain objective that is wished to be minimized, alongside other constraints that might be imposed in the system. A classical example of topology optimization is the so called binary compliance problem, in which regions of solid and void material are distributed inside a volume, with the intention of designing a structural component that will be able to withstand certain loads applied to its boundaries, but that will have the least amount of deformation possible. Additionally, this structure should at most use a specified fraction of its design volume, or its total weight must be kept within a certain limit. We can express this specific problem mathematically as:

$$\begin{aligned} \text{minimize} \quad & c(\boldsymbol{\rho}) = \boldsymbol{F}^T \boldsymbol{U} && (2.1) \\ \text{subject to} \quad & \boldsymbol{K}(\boldsymbol{\rho})\boldsymbol{U} = \boldsymbol{F} && (2.2) \\ & V = \sum_{i \in \mathbb{N}_e} \rho_i v_i \leq V_c && (2.3) \\ & 0 \leq \rho_{min} \leq \rho_i \leq 1, \quad \forall i \in \mathbb{N}_e && (2.4) \end{aligned}$$

where in equation 2.1 the objective function that is to be minimized is given by $c(\boldsymbol{\rho}) = \boldsymbol{F}^T \boldsymbol{U}$, where $\rho$ takes the value 0 or 1 depending on whether our small region in space is empty or contains material, $\boldsymbol{U}$ is the displacement of piece of material, $\boldsymbol{F}$ is the force applied to it, and $\mathbb{N}_e$ is a finite set of elements inside the design domain $\Omega$. The quantity $c$ is referred to as compliance, and physically it is the inverse of the stiffness of the structure. The deformation of this material in the design domain is controlled by Hooke's Law, which is shown in equation 2.2. $\boldsymbol{K}(\boldsymbol{\rho})$ is defined as a global stiffness matrix [19]

$$\boldsymbol{K}(\boldsymbol{\rho}) = \sum_{i \in \mathbb{N}_e} \boldsymbol{K}_i(\rho_i) \tag{2.5}$$

where $\rho_i$ is the density at each region $i$, and we assemble all those densities into the vector $\boldsymbol{\rho}$.

More generally, the formulation of topology optimization can be written as a minimization problem over a domain subject to one or more constraints, where the quantity that is being minimized is called the objective function. This objective function in turn could be an assembly of sub-objectives, each with its own relative weight with respect to the final solution. The minimized quantity is also written as a function of the design variables, which in most topology optimization problems refers to the amount of material that is present in a small region of the design domain. Additionally, we might impose an upper limit of the total amount of volume used. This was shown in equation 2.3, where the maximum allowed volume fraction of the design domain $\Omega$ is denoted as $V_c$. Mathematically, the generalized problem of topology optimization can be formulated as follows:

$$\begin{aligned} \text{minimize} \quad & X_{obj} = w_1 O_1 + w_2 O_2 + ... + w_m O_m \\ \text{subject to} \quad & \text{governing equations} \\ & V = \sum_{i \in \mathbb{N}_e} \rho_i v_i \leq V_c \\ & 0 \leq \rho_{min} \leq \rho_i \leq 1, \quad \forall i \in \mathbb{N}_e \\ & w_1 + w_2 + ... + w_m = 1 \end{aligned} \tag{2.6}$$

where $O_1, O_2, ..., O_m$ are the subobjectives, and $w_1, w_2, ..., w_m$ their respective relative weights.

### 2.2.2 Homogenization and SIMP

Unfortunately, the formulation above suffers from a major problem. Stated as is, the problem above is well-known to be ill-posed [20], as it is possible to obtain a chattering design with an infinite number of holes of infinitesimal size, thus rendering this com-

pliance problem to be unbounded [21]. To remedy this situation, several approaches have been proposed in the literature. One approach to control the chattering design is ensure that the total perimeter of the resulting structure has an upper bound [22] [23], but this e method suffers from several complications in implementation, and small variations in the parameters of the algorithm can lead to wildly different designs of the final structure [23].

A different alternative would be the utilization of a homogenization method [24], [25] [26] in which the binary representation of the material within the design domain is relaxed and intermediate values of densities are allowed, instead of just allowing empty and filled-values. One of the difficulties with using the homogenization method is how to interpret the intermediate densities of the material. In topology optimization problem involving the design of fluid flow media, the minimum value of the density could be interpreted as a fluid, the maximum value could be interpreted as a solid, while intermediate values could be interpreted as porous media [27]. In structural problems, intermediate values could be interpreted as periodic composite materials with high-resolution microscopic features [28] [29], materials that are composed of lattice structures [30], or even complex structures consisting of anisotropic fiber-reinforced composite materials [31]. Although the homogenization method is successful in solving the chattering design problem, validation of the resulting topologies using most Finite Element Method (FEM) software is very computationally expensive, since the resulting microstructures requires very fine meshes with high number of elements and nodes [32]. Additionally, the use of microstructures can also lead to stress amplifications which need to be managed appropriately to avoid regions of high stress concentration that might compromise the stability or functionality of the manufactured part [33]. It is also worthy of note that when this method was introduced back in the 1980's, manufacturability of components designed with the homogenization method was not feasible, as it was very difficult to manufacture components with microstructures or lattices. Nevertheless, the recent progress of additive manufacturing has revived the interest for structures with microstructures due to their newfound manufacturability [34].

A simpler method that tries to avoid the complications of homogenization theory is the Solid Isotropic Material Penalization method (SIMP), which utilizes yet another continuous density function. The main point of SIMP is to apply a power-law interpolation function to the material density, with the objective to penalize intermediate densities and drive them to their extreme values of void and full material. [35] [36]. This method was beneficial at the time this method was being developed in the late 80's and 90's, since as previously mentioned, it was yet fairly difficult to manufacture parts with complicated microstructures, and thus methods that drove densities to a binary result of void and material were preferred. Additionally, since the implementation of this method is simpler and less computationally intensive than homogenization, many modern FEM software use SIMP for topology optimization [37].

To understand its implementation, let us return to the problem of the design of a support structure by minimizing its compliance (equations 2.1 - 2.4). Since the material density is allowed to take intermediate values, the same applies for the structure's mechanical properties, and therefore Young's modules could be computed using the following power law:

$$E_i = E_i(\rho_i) = \rho_i^p E_i, \tag{2.7}$$

where $E_i$ is the modulus of elasticity at a region i of the design domain $\Omega$, $\rho_i$ is the density field at that region $i$, $E_0$ is the modulus of elasticity of the solid material and $p$ is the penalization factor that tries to drive the density towards its binary void and solid values. However, since the SIMP method is usually used in conjunction with FEM to solve for the density distribution, it is required to avoid void material configurations that would result in singularities during the numerical computation steps. Instead, we can rewrite equation 2.7 as:

$$E_i = E_i(\rho_i) = E_{min} + \rho_i^p (E_0 - E_{min}), \tag{2.8}$$

in which the addition of the $E_min$ avoids singularities, and $E_0$ can be chosen to be

small to represent regions of void material.

### 2.2.3 Filtering techniques

Unfortunately, usage of the SIMP method as stated in 2.8 can also result in checkerboard patterns or might add very thin details that are comparable in size to the mesh size, causing the final result to converge to a very different topology depending on the of the length scale of the mesh [38]. One of the possible techniques in the literature used to solve this problem is the use of filtering techniques on the density field. The main idea of these filtering techniques is to modify the density field at a point so that it becomes a weighted average of the densities of its neighboring points. Using this idea, a new filtered density field can be mathematically defined using the following equation [21]:

$$\bar{\rho_i} = \frac{\sum_{j \in N_i} H_{ij} v_j \rho_j}{\sum_{j \in N_i} H_{ij} v_j}, \tag{2.9}$$

where $\rho_j$ is the density field at a small region $j$ of the design domain $\Omega$,$v_j$ is the total volume of the region in consideration, and $N_i$ is a neighboring region around $v_j$. The term $H_ij$ is the weighing function, and it is analogous to a kernel, or convolution matrix, that is used in image processing applications to modify the properties of a pixel based on its surroundings, and that is typically used to blur, sharpen, emboss or perform other transformations to the image used (i.e. an image filtering function). $H_{ij}$ could be defined as a function of the distance between the element and neighboring elements, and should be chosen so that it is linearly or exponentially decaying away from the element. A possible weighting function could be calculated as

$$H_{ij} = \max(1 - \frac{(x_j - x_i)^2 + (y_j - y_i)^2)}{r}, 0), \tag{2.10}$$

where in this example, the design domain is two-dimensional, and $x_i$ and $y_i$ is the point in consideration, and $r$ is the radius of filtration. In other literature, equation 2.10 is also expressed as [21]

$$H_{ij} = r - dist(i,j), \tag{2.11}$$

Where $dist(i,j)$ contains all the neighboring points $j$ within a distance r of point $i$.

Another alternative to using equation 2.15 is to instead define the filter implicitly using a solution to the Helmholtz partial differential equation (PDE) using homogeneous Neumann boundary conditions that are imposed on the boundary of the design domain [39]

$$\begin{aligned} -r^2\nabla^2\bar{\rho} + \bar{\rho} &= \rho \\ \frac{\partial\bar{\rho}}{\partial\boldsymbol{n}} &= 0, \end{aligned} \tag{2.12}$$

where $r$ is the filter radius. The solution of this equation is a function that decays monotonically as is desired, and also preserves the volume of the design domain after the filtering process is completed. Additionally, equation 2.12 can be solved within the same finite element solver that is utilized for the solution of the whole topological optimization problem, and it requires no extra information beyond the mesh connectivity around each volume or mesh element [40]. It is also important to note that when the Helmholtz filter or any other filtering function is implemented into a finite element solver, the filter radius $r$ must be bigger than the mesh edge size in order to obtain mesh independent results [41].

### 2.2.4 Threshold projection

Even though filtering is effective at solving the checkerboard design pathology, the structure that is designed can also suffer from intermediate density values. To try and converge these intermediate values into a void/solid configuration, projection functions can be used to map the results of the filtered density field into 0/1. One method proposed by Xu et al. [42] is a volume-preserving, modified continuous Heaviside function

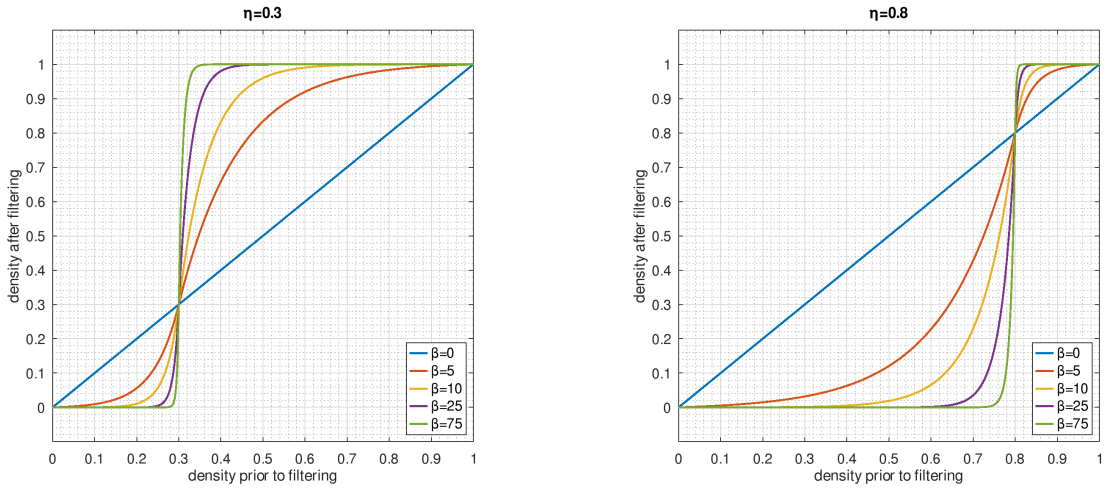


Figure 2.1: Smoothed modified Heaviside filters with $\eta = 0.3$, $\eta = 0.8$, and different values of $\beta$.

which takes the following form

$$\tilde{\rho} = \begin{cases} \eta[e^{-\beta(1-\bar{\rho}/\eta)} - (1-\bar{\rho}/\eta)e^{-\beta}] & 0 \leq \bar{\rho} \leq \eta \\ (1-\eta)[1 - e^{-\beta(\bar{\rho}-\eta)/(1-\eta)} & \\ \qquad + (\bar{\rho}-\eta)e^{-\beta}/(1-\eta)] + \eta & \eta \leq \bar{\rho} \leq 1. \end{cases} \tag{2.13}$$

In equation 2.13 $\tilde{\rho}$ is the new projected density value, $\bar{\rho}$ is the density value obtained from the Helmholtz filter function explained in the previous section, $\eta$ is a parameter that will determine where the cutoff point between the 0/1 values will be made in the x-axis, and $\beta$ will determine how fast the transition from 0/1 will be. Figure 2.1 has been included to aid the reader in understanding how the parameters affect the shape of the function.

Although the expression in equation 2.13 is successful in projecting the filtered density values, it can be replaced by a simpler and shorter expression utilizing the hyperbolic tangent function [38]

$$\tilde{\rho}_i = \frac{tanh(\beta\eta) + tanh(\beta(\bar{\rho}_i - \eta))}{tanh(\beta\eta) + tanh(\beta(1-\eta))} \tag{2.14}$$

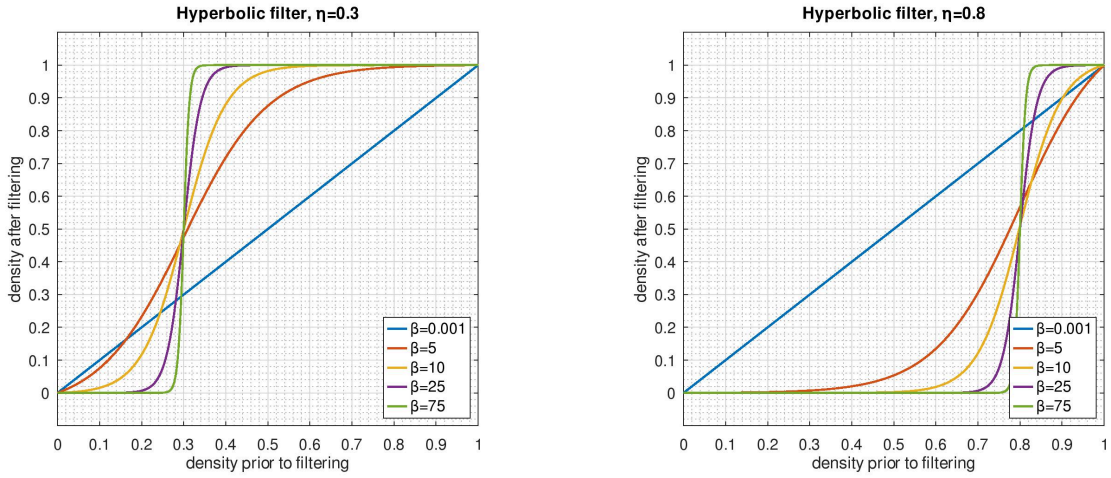


Figure 2.2: Hyberbolic tangent filter function with $\eta = 0.3$, $\eta = 0.8$, and different values of $\beta$.

Equation 2.14 has the added benefit of computing the 0/1 projection faster, and in the limit as $\beta \to \infty$ it yields the same result as equation 2.13. Plots of this equation are shown in figure 2.2.

One final point must be made before finishig this section. When a density filter is applied, the mechanical properties of the structure, such as Young's modulus or thermal conductivity, also become a function of the filtered function. For example, in the context of the structural problem described by equations 2.1 - 2.4, Young's modulus described by equation 2.8 changes into the following:

$$E_i = E_i(\tilde{\rho}_i) = E_{min} + \tilde{\rho}_i^p(E_0 - E_{min}), \tag{2.15}$$

where $\tilde{\rho}_i$ denotes the filtered density using the hyperbolic tangent filter at a small element $i$ of the design domain $\Omega$.

### 2.2.5 Final formulation of the topology optimization problem

In this work, topology optimization was utilized to design a support structure for components created by additive manufacturing. The design variables are the densities of the support structure throughout its design domain, which is the volume between the

component and the base plate. The objective function utilized was a multi-objective function that sought to simultaneously maximize heat conduction and minimize the compliance of the supporting structure. The material properties of the support structure that depend on the design variables are the thermal conductivity and Young's modulus. A Helmholtz filter was utilized, and the final density was computed using a hyperbolic tangent projection. Additionally, a volume fraction constrain was employed with the intention of reducing the amount of material used. Mathematically, all of these conditions can be represented as follows:

$$\begin{aligned}
\text{minimize} \quad & X_{obj} = w_1 \boldsymbol{F}^T \boldsymbol{U} + w_2 \boldsymbol{T}^T \boldsymbol{Q} && (2.16)\\
\text{subject to} \quad & \boldsymbol{\kappa}(\tilde{\boldsymbol{\rho}}) \boldsymbol{T} = \boldsymbol{Q} && (2.17)\\
& \boldsymbol{K}(\tilde{\boldsymbol{\rho}}) \boldsymbol{U} = \boldsymbol{F} && (2.18)\\
& V = \sum_{i \in \mathbb{N}_e} \tilde{\rho}_i v_i \leq V_c && (2.19)\\
& 0 \leq \rho_{min} \leq \tilde{\rho}_i \leq 1, \quad \forall i \in \mathbb{N}_e && (2.20)\\
& w_1 + w_2 = 1, && (2.21)
\end{aligned}$$

where $\tilde{\boldsymbol{\rho}} = [\tilde{\rho_1}, \tilde{\rho_2}, ..., \tilde{\rho_n}]^T$ and the physical densities $\tilde{\rho}_i$ are defined by equation 2.14, $\boldsymbol{U}$ denotes the nodal displacement vector, $\boldsymbol{T}$ denotes the nodal temperature vector, $\boldsymbol{F}$ is the vector of nodal forces, and $\boldsymbol{Q}$ is the thermal load vector. Equation 2.16 is the objective function, with the first term being mechanical compliance, and the second term being thermal compliance, which is the inverse of thermal conductivity.Equation 2.19 is the volume constraint equation. Equation 2.17 governs the thermal conduction of the material, with the thermal conductivity matrix $\boldsymbol{\kappa}$ calculated as:

$$\boldsymbol{\kappa}(\tilde{\boldsymbol{\rho}}) = \sum_{i \in \mathbb{N}_e} [k_{min} + \tilde{\rho}_i^p (k_0 - k_{min})] \boldsymbol{k_i^0} \tag{2.22}$$

where $k_{min}$ and $k_0$ are the element's minimum and maximum thermal conductivities,

and $\boldsymbol{k}_i^0$ is the element's conductivity matrix. On the other hand, equation 2.18 governs the deformation of the structure, with the stiffness matrix $\boldsymbol{K}$ calculated as

$$\boldsymbol{K}(\tilde{\boldsymbol{\rho}}) = \sum_{i \in \mathbb{N}_e} [E_{min} + \tilde{\rho}_i^p (E_0 - E_{min})] \boldsymbol{K_i^0} \tag{2.23}$$

with $E_{min}$ and $E_0$ denoting the limits of Young's modulus, and $\boldsymbol{K}_i^0$ is the element's stiffness matrix as defined in [21].

Additionally, the reader must note that in equations 2.22 and 2.23, $\sum$ does not denote summation, but instead the finite element assembly operator [19].

## 2.3 Summary of literature

Lee and Xie [43] developed an optimization algorithm that detects the best locations for supports in the boundaries of the design space, which can lead to an increase in stiffness and aid in minimizing deformation.

## 2.4 Research originality and contribution

# Chapter 3

# Methodology

## 3.1 Introduction

To analyze the performance of different support structures created using topology optimization, a comparison study was made in which parts created by additive manufacturing were paired with different support structures. This study assumed that different structures will conduct heat energy differently, and thus some topologies might be more effective in removing heat faster from each material layer as it is being processed. This increased thermal conduction would then result in less overall thermal deformation, as the manufactured component would expand less due to the decreased time in high temperatures.

This section will explain the full process taken to run the simulations and analyze the data. An overview of the process can be seen in Figure 3.1. The process starts from the creation of the CAD for the manufactured components, followed by the design and CAD creation of the support structures. The components and the support structures are then merged, and imported into the additive manufacturing software to simulate the results of manufacture. The results from the manufacturing simulation are then analyzed by means of graphs and statistical methods.

The subsequent sections explain in detail each stage of this process.

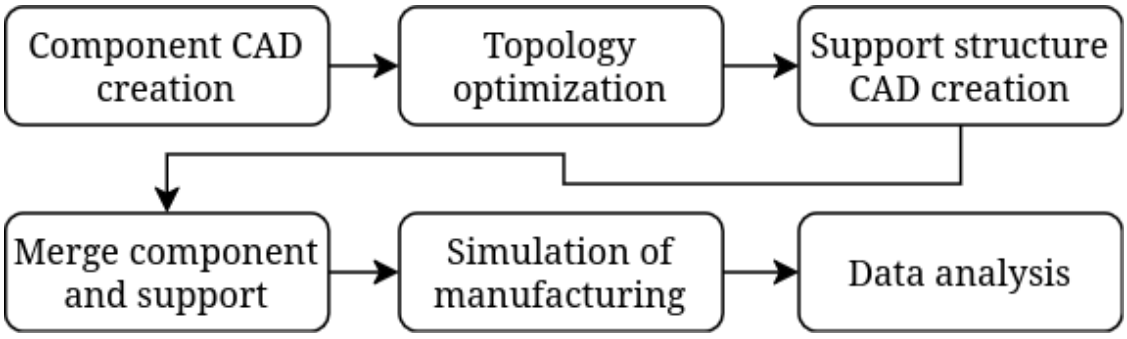


Figure 3.1: Process diagram.

## 3.2 Component CAD creation

### 3.2.1 Simple geometry

The components with simple geometries utilized in this study consist of a cube, three triangular components with different slopes, and three cylindrical components with different values of curvature. To reiterate, these components have the same dimensions that were used in the study of lattice support structure performance by Peishu **peishu_thesis**. All the CAD models used for the simple geometry study were created using FreeCAD, an open-source CAD software. All the components were expoerted as .STEP files, and then they were merged with their corresponding support structures using the software nTop.

- A cube with side length of 30 mm (Figure 3.2).
- Three triangular components with varying slopes. All triangular components have a base of 30 x 30 $mm^2$, with slopes of 15 °, 30 °and 45 °. The measurements are shown in figure.

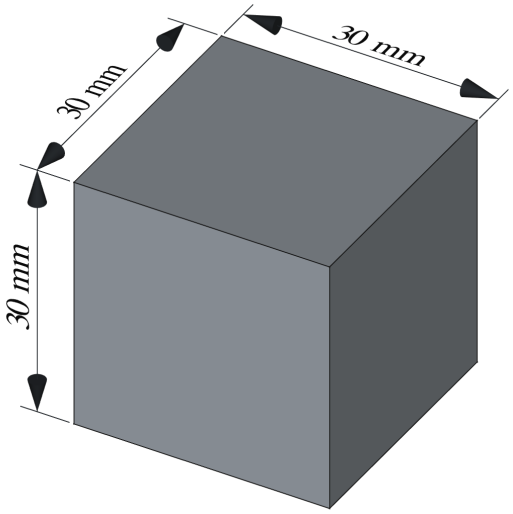


Figure 3.2: Dimensions of cube component.

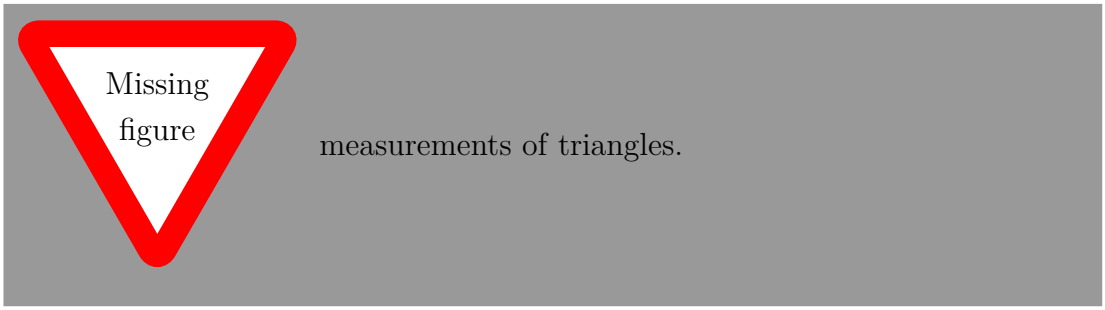


measurements of triangles.

- Add cylinders here

Add figure of cylinders

### 3.2.2 Femoral component

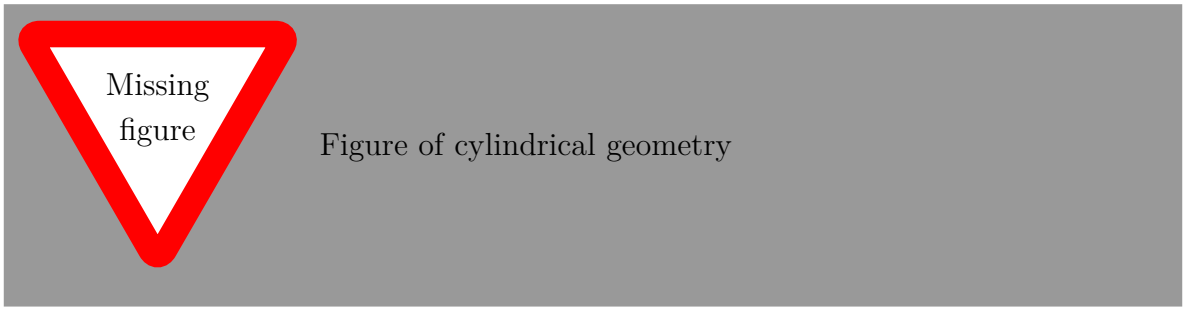


Figure of cylindrical geometry

## 3.3 Support structure creation

The supporting structures of the components were created using the method of topology optimization. The design was implemented using the topology optimization module of COMSOL Multiphysics 6.2.

The steps for creating a valid topology optimization model are: determine the design volume, choose a suitable mathematical model for the behavior of the material within the design volume, choose the objective functions and decide what constraints need to the material within the volume be applied to the design volume. The following section explains all of these steps in detail.

### 3.3.1 Design domain

need to expand on this and make it better. need to get dimesions of components

#### Simple geometry design domain

The design domain for the simple geometry components consists of the volume between the bottom face of each component and the base plate. For the cube, the design domain ends up being a rectangular prism with dimensions 10 cm x 30 cm x 30 cm. For the triangles, the design domain consists of different triangular spaces with a square base, shown in figures

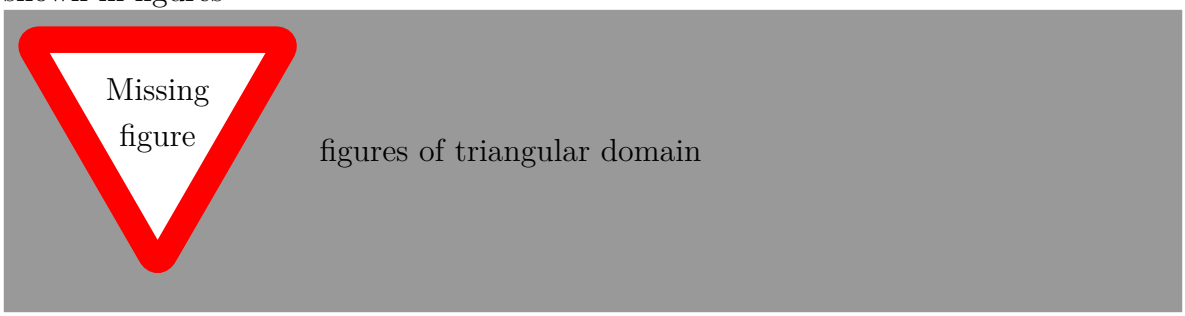


figures of triangular domain

. .

Add here the cylindrical component geometry

Since all of these components can be generated by the drawing their profile on a plane and extruding it in a direction perpendicular to the plane, the design domain utilized in the topology optimization model is also a 2D model. This grants the benefit

of faster computation, and thus the supporting structure is created by first finding the planar topology and also extruding it in a perpendicular direction.

**Femoral component design domain**

### 3.3.2 Mathematical model

The mathematical models consists of the governing equations used to describe the physics of the system and the constraints imposed on the model, as well as the objective function that needs to be minimized.

For this system, the most appropriate objective function would be the maximization of thermal conductivity; in order to minimize the thermal deformation of the manufactured component, it is imperative to transfer heat away from it as fast as possible. The physical equation describing the thermal conduction of a material is given by Fourier's Law, which can be expressed as:

$$q = -k\nabla T \tag{3.1}$$

where q is the heat conduction through the material, k is the material's thermal conductivity and $\nabla T$ is the thermal gradient.

For this study, the only constraint applied on the system was the volume fraction. Volume fraction speficies the maximum amount of volume that the designed topology should take from the design domain. The volume fractions utilized were 50% and 75%.

Write down equation of thermal conductivity for top optimiation domain here.

### 3.3.3 Objective functions

An additional objective function to be considered would be the deformation of the supporting structure as well. If the supporting structure is composed of very thin segments, there is a high possiblity that the structure might buckle, which would add significant geometric errors to the component. In the worst case scenario, the structure itself would collapse, causing the entire manufacturing process to fail. In order to

avoid this, it is necessary to limit the amount of deformation that is allowed in the support structure. This can be achieved by utilizing an aditional objective function of structural compliance minimization. We define structural compliance as the amount of energy stored in the deformation of material. Minimizing this stored energy is thus equivalent to minimizing the deformation. Therefore, the second objective function of minimization of structural compliance is also used in the topology optimization model.as heat passes into the support structure from the bottom of the manufactured component,

The next step is applying certain constriants on the system. For this study, we are mostly concerned with the principal constrain is the volume fraction, which is the maximum amount of volume that the topology can cover within the design domain. This criteria is chosen because we seek to use less material for the supporting structure, as long as we can maintain the total deformation of the manufacturing componont beneath a threshold. For the model in COMSOL, the values of volume fraction = 0.5 and volume fraction = 0.75 were used.

probably want to add a reference to this somewhere.

Write equation of compliance here

Merge them together to get the final objective function. Explain about the weights.

Talk about Helmholtz filter

Hyperbolic tangent

### 3.3.4 COMSOL implementation

**Mesh**

**Physical parameters**

**Simulation itself**

As discussed in the previous chapter, Helmholtz filters are frequently used in topology optimization studies to avoid chattering designs.

## 3.4 Component and support structure merging

### 3.4.1 CAD for support structure

This section talks about how FreeCAD was used to create the support structure once the pictures of the topolgies have been obtained.

### 3.4.2 Merging of part with support structure

Once the CAD file of the component and the support structure has been built, it is necessary to merge them together and import them into Simufact to undergo simulation of the manufacturing process. The software used for blending the component and its support structure is nTop . nTop's interface makes it very easy to merge the part, and also allows to blend the support structure and the component, which effectively creates a fillet between the nodes of both components to allow for a smooth transition between bodies. Of course, blending the component and the support structure in this manner would not give any benefit in a real manufacturing process, as the structure and the component would not be able to be separated easily. NEvertheless, this blend radius is beneficial for the simulation since it was observed that a direct union and import of the support structure + component in Simufact resulted in having very small gaps between the two pieces, resulting in a non manifold geometry that would cause the finite element model to have gaps between some of its nodes.

add version here


add figure of error / warning from Simufact due to import of structure with gaps. Two figures should suffice here.

## 3.5 Simulation of manufacturing process

The software utilized to simulate the manufacturing process is Simufact Additive version 2023.2. Simufact Additive is capable of simulation building process of additive manufacturing components, and coupling thermal and stress physics to predict the temperature values of the component throughout the building process and the total stresses, strains and deformations resulting from the manufacturing process.

In order to set up Simufact correctly, the building process and the building space

geometry must be specified before each simulation. The building parameters and building geometries used in this study are the same that were used in the analysis of thermal deformation using lattice support structures done by Peihsy and al.

add reference here

### 3.5.1 Simufact simulation parameters and voxelization

add that thermo-mechanical process was used and explain what it is.

After the component and the support structures were merged, they were imported into Simufact. It is during this step that all the factors related to the simulation are set, which include the machine properties, material properties, and build parameters. As mentioned previously, these were chosen to be identical to the study of PeiHsu to ensure that the results of this study could be compared to the results of that one.

The first parameter to be chosen is the process properties, which determines the physics that Simufact takes into consideration to run the simulation. Simufact provides three different types of processes: mechanical, thermal, and thermomechanical. As stated in the Simufact manual , mechanical provides a fast mechanical analysis that only uses inherent strains as the main input. This type of analysis does not take into consideration the temperature fields during the building process. The thermal process on the other hand only considers the thermal behaviour of the components, and the temperature field of the support structures, components and base can be analyzed. The thermomechanical process couples the stress and thermal analyses, and allows for the prediction of temperature, distortions and stresses of the part. This latter process is the one used in this study.

insert reference to manual here

After choosing the process property, the machine parameters must be specified. This includes the machine build plate geometry and the laser parameters. The machine build plate chosen was a circular plate with an 80 mm radius. The build space dimensions consists of a space of 160 mm in all three x-y-z directions. As for the laser parameters, the simulations were carried out with one laser with a maximum laser power of 500 W and a maximum laser speed of 2000 mm / s, an efficiency of 25 percent, and a beam width of 25 mm. All of these parameters are summarized in the table

add the table of building parameters here.

The building parameters for the process need also to be set. These include material layer parameters and any thermal parameters and temperature specifications for the build environment and base plate. The powder layer thickness was chosen to be 0.03 mm, with a recoater time of 10 s. The powder initial temperature was set to 25 °Celcius, with an initial base temperature of 200 degrees.

explain why base plate temepra-ture might be used in practice, might want to add reference to 10.3390/therm

### 3.5.2 Convergence analysis

To make sure that the results of the simulation would not depend on the voxel density of the

## 3.6 Data collection and organization

*This section will detail how I collected the data from Simufact and what software and methods I used to organize it an analyze it. The actual results will go in the following chapter, aptly named results, duh*

Need to add expo-sure time, exposure energy frac-tion, and volumet-ric expan-sion factors here. Need to refer to Comsol documenta-tion to ex-plain what these are and how they influ-

# Todo list

# References


[1] M. A. Varacallo, T. D. Luo, A. Mabrouk, and N. A. Johanson, "Total Knee Arthroplasty Techniques," in *StatPearls*, Treasure Island (FL): StatPearls Publishing, 2025. pmid: 29763071. Accessed: Feb. 11, 2025. [Online]. Available: http://www.ncbi.nlm.nih.gov/books/NBK499896/.

[2] "Elderly and disadvantaged situation, trend and strategy analysis of living environment in Taiwan," Architecture and Building Research Institute, Ministry of the Interior, ROC (Taiwan), Accessed: Feb. 11, 2025. [Online]. Available: http://www.abri.gov.tw/en/News_Content.aspx?n=908&s=317737&sms=9518.

[3] F.-H. Lin et al., "The increase in total knee replacement surgery in Taiwan," *Medicine*, vol. 97, no. 31, e11749, Aug. 3, 2018, ISSN: 0025-7974. DOI: 10.1097/MD.0000000000011749. pmid: 30075592. Accessed: Feb. 11, 2025. [Online]. Available: https://www.ncbi.nlm.nih.gov/pmc/articles/PMC6081077/.

[4] S. P. Narra, P. N. Mittwede, S. DeVincent Wolf, and K. L. Urish, "Additive Manufacturing in Total Joint Arthroplasty," *The Orthopedic clinics of North America*, vol. 50, no. 1, pp. 13–20, Jan. 2019, ISSN: 0030-5898. DOI: 10.1016/j.ocl.2018.08.009. pmid: 30477702. Accessed: Feb. 11, 2025. [Online]. Available: https://www.ncbi.nlm.nih.gov/pmc/articles/PMC6555404/.

[5] A. D. Valino, J. R. C. Dizon, A. H. Espera, Q. Chen, J. Messman, and R. C. Advincula, "Advances in 3D printing of thermoplastic polymer composites and nanocomposites," *Progress in Polymer Science*, vol. 98, p. 101 162, Nov. 1, 2019, ISSN: 0079-6700. DOI: 10.1016/j.progpolymsci.2019.101162. Accessed:

Feb. 27, 2025. [Online]. Available: https://www.sciencedirect.com/science/article/pii/S0079670018303976.

[6] M. Marsh and S. Newman, "Trends and developments in hip and knee arthroplasty technology," *Journal of Rehabilitation and Assistive Technologies Engineering*, vol. 8, p. 2 055 668 320 952 043, Feb. 8, 2021, ISSN: 2055-6683. DOI: 10.1177/2055668320952043. pmid: 33614108. Accessed: Feb. 17, 2025. [Online]. Available: https://www.ncbi.nlm.nih.gov/pmc/articles/PMC7874345/.

[7] M. H. Mobarak et al., "Recent advances of additive manufacturing in implant fabrication –A review," *Applied Surface Science Advances*, vol. 18, p. 100 462, Dec. 1, 2023, ISSN: 2666-5239. DOI: 10.1016/j.apsadv.2023.100462. Accessed: Feb. 17, 2025. [Online]. Available: https://www.sciencedirect.com/science/article/pii/S266652392300096X.

[8] K. Pathak et al., "3D printing in biomedicine: Advancing personalized care through additive manufacturing," *Exploration of Medicine*, vol. 4, no. 6, pp. 1135–1167, 6 Dec. 29, 2023, ISSN: 2692-3106. DOI: 10.37349/emed.2023.00200. Accessed: Feb. 17, 2025. [Online]. Available: https://www.explorationpub.com/Journals/em/Article/1001200.

[9] A. M. Jonaet, H. S. Park, and L. C. Myung, "Prediction of residual stress and deformation based on the temperature distribution in 3D-printed parts," *The International Journal of Advanced Manufacturing Technology*, vol. 113, no. 7, pp. 2227–2242, 7 Apr. 1, 2021, ISSN: 1433-3015. DOI: 10.1007/s00170-021-06711-5. Accessed: Mar. 1, 2025. [Online]. Available: https://link-springer-com.proxyone.lib.nchu.edu.tw:8443/article/10.1007/s00170-021-06711-5.

[10] R. E. Laureijs and J. B. Rocca. "Metal Additive Manufacturing: Cost Competitive Beyond Low Volumes | J. Manuf. Sci. Eng. | ASME Digital Collection," Accessed: Feb. 11, 2025. [Online]. Available: https://asmedigitalcollection.asme.org/

manufacturingscience/article/139/8/081010/376354/Metal-Additive-Manufacturing-Cost-Competitive.

[11] Chung, Pei-Hsu, "Study on the Lattice Support Structures to Minimize Thermal Distortion in Selective Laser Melting Using Simulation and Design of Experiments," 國立中興大學, 臺中市, 2024.

[12] G. Allaire and B. Bogosel, "Optimizing supports for additive manufacturing," *Structural and Multidisciplinary Optimization*, vol. 58, no. 6, pp. 2493–2515, 6 Dec. 1, 2018, ISSN: 1615-1488. DOI: 10.1007/s00158-018-2125-x. Accessed: Feb. 20, 2025. [Online]. Available: https://link-springer-com.proxyone.lib.nchu.edu.tw:8443/article/10.1007/s00158-018-2125-x.

[13] Y.-H. Kuo, C.-C. Cheng, Y.-S. Lin, and C.-H. San, "Support structure design in additive manufacturing based on topology optimization," *Structural and Multidisciplinary Optimization*, vol. 57, no. 1, pp. 183–195, 1 Jan. 1, 2018, ISSN: 1615-1488. DOI: 10.1007/s00158-017-1743-z. Accessed: Feb. 20, 2025. [Online]. Available: https://link-springer-com.proxyone.lib.nchu.edu.tw:8443/article/10.1007/s00158-017-1743-z.

[14] H. A. Kumar, P. F. Reginald Elvis, M. Manoharan, J. Jayapal, and S. Kumaraguru, "Tailored Support Structures for Additive Manufacturing," in *Advances in Additive Manufacturing and Joining*, ser. Lecture Notes on Multidisciplinary Industrial Engineering, Singapore: Springer, 2020, pp. 199–207, ISBN: 978-981-329-432-5. DOI: 10.1007/978-981-32-9433-2_17.

[15] M. Zhou, Y. Liu, and Z. Lin, "Topology optimization of thermal conductive support structures for laser additive manufacturing," *Computer Methods in Applied Mechanics and Engineering*, vol. 353, pp. 24–43, Aug. 15, 2019, ISSN: 0045-7825. DOI: 10.1016/j.cma.2019.03.054. Accessed: Feb. 20, 2025. [Online]. Available: https://www.sciencedirect.com/science/article/pii/S0045782519301938.

[16] M. P. Bendsøe and O. Sigmund, *Topology Optimization*, 2nd ed. Springer Berlin, Heidelberg, Oct. 10, 2002, XIV, 370, ISBN: 978-3-540-42992-0.

[17] J. Ye et al., "Topology optimisation of self-supporting structures based on the multi-directional additive manufacturing technique," *Virtual and Physical Prototyping*, vol. 18, no. 1, e2271458, Dec. 31, 2023, ISSN: 1745-2759, 1745-2767. DOI: 10.1080/17452759.2023.2271458. Accessed: Feb. 20, 2025. [Online]. Available: https://www.tandfonline.com/doi/full/10.1080/17452759.2023.2271458.

[18] M. Langelaar, "TOPOLOGY OPTIMIZATION FOR ADDITIVE MANUFACTURING WITH CONTROLLABLE SUPPORT STRUCTURE COSTS," in *Proceedings of the VII European Congress on Computational Methods in Applied Sciences and Engineering (ECCOMAS Congress 2016)*, Crete Island, Greece: Institute of Structural Analysis and Antiseismic Research School of Civil Engineering National Technical University of Athens (NTUA) Greece, 2016, pp. 3689–3699, ISBN: 978-618-82844-0-1. DOI: 10.7712/100016.2065.5873. Accessed: Feb. 20, 2025. [Online]. Available: http://www.eccomasproceedia.org/conferences/eccomas-congresses/eccomas-congress-2016/2065.

[19] G. Hornberger and P. Wiberg, "The Finite Element Method: An Introduction," in *Numerical Methods in the Hydrological Sciences*, American Geophysical Union (AGU), 2005, pp. 1–10, ISBN: 978-1-118-70952-8. DOI: 10.1002/9781118709528.ch10. Accessed: Feb. 24, 2025. [Online]. Available: https://onlinelibrary.wiley.com/doi/abs/10.1002/9781118709528.ch10.

[20] R. V. Kohn and G. Strang, "Optimal design and relaxation of variational problems, I," *Communications on Pure and Applied Mathematics*, vol. 39, no. 1, pp. 113–137, Jan. 1986, ISSN: 0010-3640, 1097-0312. DOI: 10.1002/cpa.3160390107. Accessed: Feb. 24, 2025. [Online]. Available: https://onlinelibrary.wiley.com/doi/10.1002/cpa.3160390107.

[21] K. Liu and A. Tovar, "An efficient 3D topology optimization code written in Matlab," *Structural and Multidisciplinary Optimization*, vol. 50, no. 6, pp. 1175–

1196, Dec. 2014, ISSN: 1615-147X, 1615-1488. DOI: 10.1007/s00158-014-1107-x. Accessed: Dec. 17, 2023. [Online]. Available: http://link.springer.com/10.1007/s00158-014-1107-x.

[22] R. B. Haber, C. S. Jog, and M. P. Bendsøe, "A new approach to variable-topology shape design using a constraint on perimeter," *Structural optimization*, vol. 11, no. 1, pp. 1–12, Feb. 1, 1996, ISSN: 1615-1488. DOI: 10.1007/BF01279647. Accessed: Sep. 12, 2024. [Online]. Available: https://doi.org/10.1007/BF01279647.

[23] C. S. Jog, "Topology design of structures using a dual algorithm and a constraint on the perimeter," *International Journal for Numerical Methods in Engineering*, vol. 54, no. 7, pp. 1007–1019, 2002, ISSN: 1097-0207. DOI: 10.1002/nme.457. Accessed: Feb. 24, 2025. [Online]. Available: https://onlinelibrary.wiley.com/doi/abs/10.1002/nme.457.

[24] M. P. Bendsøe, *Optimization of Structural Topology, Shape, and Material*. Berlin, Heidelberg: Springer, 1995, ISBN: 978-3-662-03117-9 978-3-662-03115-5. DOI: 10.1007/978-3-662-03115-5. Accessed: Feb. 24, 2025. [Online]. Available: http://link.springer.com/10.1007/978-3-662-03115-5.

[25] G. Allaire, *Shape Optimization by the Homogenization Method* (Applied Mathematical Sciences), S. S. Antman, J. E. Marsden, and L. Sirovich, red. New York, NY: Springer, 2002, vol. 146, ISBN: 978-1-4419-2942-6 978-1-4684-9286-6. DOI: 10.1007/978-1-4684-9286-6. Accessed: Feb. 24, 2025. [Online]. Available: http://link.springer.com/10.1007/978-1-4684-9286-6.

[26] K. Suzuki and N. Kikuchi, "A homogenization method for shape and topology optimization," *Computer Methods in Applied Mechanics and Engineering*, vol. 93, no. 3, pp. 291–318, Dec. 1, 1991, ISSN: 0045-7825. DOI: 10.1016/0045-7825(91)90245-2. Accessed: Feb. 24, 2025. [Online]. Available: https://www.sciencedirect.com/science/article/pii/0045782591902452.

[27] M. Pietropaoli, F. Montomoli, and A. Gaymann, "Three-dimensional fluid topology optimization for heat transfer," *Structural and Multidisciplinary Optimization*, vol. 59, no. 3, pp. 801–812, Mar. 1, 2019, ISSN: 1615-1488. DOI: 10.1007/s00158-018-2102-4. Accessed: Dec. 21, 2024. [Online]. Available: https://doi.org/10.1007/s00158-018-2102-4.

[28] J. P. Groen and O. Sigmund, "Homogenization-based topology optimization for high-resolution manufacturable microstructures," *International Journal for Numerical Methods in Engineering*, vol. 113, no. 8, pp. 1148–1163, Feb. 24, 2018, ISSN: 0029-5981, 1097-0207. DOI: 10.1002/nme.5575. Accessed: Feb. 24, 2025. [Online]. Available: https://onlinelibrary.wiley.com/doi/10.1002/nme.5575.

[29] J. Alexandersen and B. S. Lazarov, "Topology optimisation of manufacturable microstructural details without length scale separation using a spectral coarse basis preconditioner," *Computer Methods in Applied Mechanics and Engineering*, vol. 290, pp. 156–182, Jun. 15, 2015, ISSN: 0045-7825. DOI: 10.1016/j.cma.2015.02.028. Accessed: Feb. 24, 2025. [Online]. Available: https://www.sciencedirect.com/science/article/pii/S0045782515000924.

[30] G. Allaire, P. Geoffroy-Donders, and O. Pantz, "Topology optimization of modulated and oriented periodic microstructures by the homogenization method," *Computers & Mathematics with Applications*, Simulation for Additive Manufacturing, vol. 78, no. 7, pp. 2197–2229, Oct. 1, 2019, ISSN: 0898-1221. DOI: 10.1016/j.camwa.2018.08.007. Accessed: Feb. 24, 2025. [Online]. Available: https://www.sciencedirect.com/science/article/pii/S0898122118304255.

[31] D. Kim, J. Lee, T. Nomura, E. M. Dede, J. Yoo, and S. Min, "Topology optimization of functionally graded anisotropic composite structures using homogenization design method," *Computer Methods in Applied Mechanics and Engineering*, vol. 369, p. 113 220, Sep. 1, 2020, ISSN: 0045-7825. DOI: 10.1016/j.

cma.2020.113220. Accessed: Feb. 24, 2025. [Online]. Available: https://www.sciencedirect.com/science/article/pii/S0045782520304059.

[32] J.-E. Kim, N.-K. Cho, and K. Park, "Computational homogenization of additively manufactured lightweight structures with multiscale topology optimization," *Journal of Computational Design and Engineering*, vol. 9, no. 5, pp. 1602–1615, Sep. 8, 2022, ISSN: 2288-5048. DOI: 10.1093/jcde/qwac078. Accessed: Feb. 24, 2025. [Online]. Available: https://academic.oup.com/jcde/article/9/5/1602/6660651.

[33] G. Allaire, F. Jouve, and H. Maillot, "Topology optimization for minimum stress design with the homogenization method," *Structural and Multidisciplinary Optimization*, vol. 28, no. 2, pp. 87–98, Sep. 1, 2004, ISSN: 1615-1488. DOI: 10.1007/s00158-004-0442-8. Accessed: Feb. 24, 2025. [Online]. Available: https://doi.org/10.1007/s00158-004-0442-8.

[34] G. Allaire, L. Cavallina, N. Miyake, T. Oka, and T. Yachimura, "The Homogenization Method for Topology Optimization of Structures: Old and New," *Interdisciplinary Information Sciences*, vol. 25, no. 2, pp. 75–146, 2019. DOI: 10.4036/iis.2019.B.01.

[35] M. P. Bendsøe, "Optimal shape design as a material distribution problem," *Structural optimization*, vol. 1, no. 4, pp. 193–202, Dec. 1, 1989, ISSN: 1615-1488. DOI: 10.1007/BF01650949. Accessed: Feb. 24, 2025. [Online]. Available: https://doi.org/10.1007/BF01650949.

[36] G. I. N. Rozvany, M. Zhou, and T. Birker, "Generalized shape optimization without homogenization," *Structural optimization*, vol. 4, no. 3, pp. 250–252, Sep. 1, 1992, ISSN: 1615-1488. DOI: 10.1007/BF01742754. Accessed: Feb. 24, 2025. [Online]. Available: https://doi.org/10.1007/BF01742754.

[37] "SIMP Method for Topology Optimization - 2019 - SOLIDWORKS Help," Accessed: Feb. 24, 2025. [Online]. Available: https://help.solidworks.com/2019/english/SolidWorks/cworks/c_simp_method_topology.htm.

[38] F. Wang, B. S. Lazarov, and O. Sigmund, "On projection methods, convergence and robust formulations in topology optimization," *Structural and Multidisciplinary Optimization*, vol. 43, no. 6, pp. 767–784, Jun. 2011, ISSN: 1615-147X, 1615-1488. DOI: 10.1007/s00158-010-0602-y. Accessed: Feb. 25, 2025. [Online]. Available: https://link.springer.com/10.1007/s00158-010-0602-y.

[39] B. S. Lazarov and O. Sigmund, "Filters in topology optimization based on Helmholtz-type differential equations," *International Journal for Numerical Methods in Engineering*, vol. 86, no. 6, pp. 765–781, 2011, ISSN: 1097-0207. DOI: 10.1002/nme.3072. Accessed: Sep. 14, 2024. [Online]. Available: https://onlinelibrary-wiley-com.proxyone.lib.nchu.edu.tw:8443/doi/abs/10.1002/nme.3072.

[40] A. B. Lambe and A. Czekanski, "Topology optimization using a continuous density field and adaptive mesh refinement," *International Journal for Numerical Methods in Engineering*, vol. 113, no. 3, pp. 357–373, Jan. 20, 2018, ISSN: 0029-5981, 1097-0207. DOI: 10.1002/nme.5617. Accessed: Feb. 25, 2025. [Online]. Available: https://onlinelibrary.wiley.com/doi/10.1002/nme.5617.

[41] "Performing Topology Optimization with the Density Method," COMSOL, Accessed: Feb. 25, 2025. [Online]. Available: https://www.comsol.com/blogs/performing-topology-optimization-with-the-density-method.

[42] S. Xu, Y. Cai, and G. Cheng, "Volume preserving nonlinear density filter based on heaviside functions," *Structural and Multidisciplinary Optimization*, vol. 41, no. 4, pp. 495–505, 4 Apr. 1, 2010, ISSN: 1615-1488. DOI: 10.1007/s00158-009-0452-7. Accessed: Feb. 27, 2025. [Online]. Available: https://link-springer-com.proxyone.lib.nchu.edu.tw:8443/article/10.1007/s00158-009-0452-7.

[43] T.-U. Lee and Y. M. Xie, "Simultaneously optimizing supports and topology in structural design," *Finite Elements in Analysis and Design*, vol. 197, p. 103 633, Dec. 1, 2021, ISSN: 0168-874X. DOI: 10.1016/j.finel.2021.103633. Accessed:

Feb. 20, 2025. [Online]. Available: https://www.sciencedirect.com/science/article/pii/S0168874X21001177.